Journal of ELECTRICAL ENGINEERING, VOL. 57, NO. 5, 2006, 276–284

COMPARISON OF MAPMAKING METHODS FOR MOBILE ROBOTS

Jaroslav Hanzel — Ladislav Jurišica *

The problem of creating the map of an unknown environment by mobile robot control system is considered using range readings obtained by ultrasonic range finder. A grid-based representation of a robot working space is chosen. The goal is the determination of occupied and empty areas in the working environment, which is not a simple problem due the uncertainty introduced by the sensory system. Three different algorithms for map generation based on probability theory, the Dempster–Shafer theory of evidence and fuzzy set theory are compared. Experimental examples of occupancy grids, built from real data recorded in an office-like environment, are presented.

K e y w o r d s: ultrasonic sensor, occupancy grid

1 INTRODUCTION

Fully autonomous performance of given tasks by mobile robots is the main goal of recent investigation in the field of mobile robotics [1, 4]. The interest is focused on the problem of generating a working environment representation for the navigation tasks. The robot motion over a trajectory is considered. At the same time the robot collects data from its sensory system. The most common sensors [1], like the sonars and laser-scanners, detect the distance to an obstacle within range of the sensor by sending out a signal and measuring the time till the echo of the signal returns. In the majority of occasions the signal will bounce against the nearest obstacle in the direction of the sensor and therefore the measured distance will be the distance to the nearest obstacle. Of course, there are some reasons for measurement failures, and thus the measured distance is generally erroneous. The acquired distance can be used by many ways. One of them is the creation of the environment representation, which is in principle a map of the environment.

The ultrasonic range finders (sonars) are today widely used for measuring relative distances in many technical domains [1]. They have a very broad possibility of exploitation due to their simplicity of operation, low cost and modest realisation. In mobile robotics the sonars are used for measuring distances to the obstacles in the robot neighbourhood. In spite of all the advances the application of ultrasonic sensors for the creation of the robot environment representation is linked with a variety of problems. These rise from the physical principle of their operation. The ultrasonic range finders work according to a simple principle: a packet of ultrasonic waves is generated and the resulting echo is detected. The time elapsed between a transmission and a reception is assumed to be proportional to the distance of the sensed obstacle. Thereafter, we will refer to a Polaroid ultrasonic ranging system widely used in mobile robotics [7].

There are basically three main sources of measurement uncertainty in the process of determination of an object presence and its relative distance with the ultrasonic sensors. First, the measured distance r is affected by an error. In the case of the Polaroid range finder, which can detect distances from 0.15 to 10.7 m, the error of measurement is about $\pm 1\,\%$ of the measured distance over the entire range [7]. This uncertainty is caused by the characteristics of air such as its temperature, humidity, turbulence and pressure [9]. The second uncertainty results from the propagation of the ultrasonic signal to the space in the form of a cone with an axis in the scanning direction. So the exact angular position of the object reflecting the echo might not be determined, because it may occur somewhere along the arc with the radius of the measured distance. The angle of radiation can be in fact fairly wide. The transducer can be treated as a plane circular piston in order to analyse its radiation characteristics, which is given by the radiation directivity function [7]

$$P(\vartheta) = 2\frac{J_1(ka\sin\vartheta)}{(ka\sin\vartheta)}\,, \tag{1}$$

where J_1 is the Bessel function of the first order, $k = 2\pi/l$ is the wave number dependent on the wavelength l, a is the piston radius and ϑ is the azimuthal angle measured with respect to the beam's central axis. For our sensor are the valid values $a = 0.01921$ m and $l = c/f$, where c is the sound speed in air and $f = 49.410$ kHz. For practical purposes it is sufficient to take into account only the principal lobe of the transmission pattern. As a consequence a diffusion of a waves over a radiation cone of 25° width is considered. The third source of uncertainty is a phenomenon of *multiple reflections*, which may occur in the case that the incidence angle of signal to the obstacle

* Department of Automation and Control, Faculty of Electrical Engineering and Information Technology, Slovak University of Technology, Ilkovičova 3, 812 19 Bratislava. E-mail: hanzel@elf.stuba.sk

ISSN 1335-3632

is larger than a so-called *critical angle*, which is strongly dependent on the surface characteristics. In this case the reflection of the signal is mainly specular and the sensor may receive the ultrasonic beam after multiple reflections, what is called a *long reading*, or it may even get lost. Therefore, in order to return a significant range reading, the angle of incidence on the object surface has to be smaller than the critical angle.

2 MAPBUILDING ALGORITHMS

The occupancy grids provide an effective framework for the data fusion from multiple sensors and sensing positions. When a sensor reading is taken, the sensor model is overlaid on the grid, and each cell is updated. Occupancy grids are mostly used for 2-D representation of the floor plan of a scene. Each cell of grid represents some area and contains information about the space that it represents.

Consider a two-dimensional environment U discretized for computational reasons into bitmap structure of finite number of square elements called cells with size of edge δ. The set U can be formally written as $U = \{c_1, \ldots, c_M\}$ for $j = 1, \ldots, M$. Next we assume a set of range readings $R = \{r_1, \ldots, r_n\}$, collected at known locations $L = \{l_1, \ldots, l_k\}$. In principle, the task of map generating subsystem of robots control system is to process the range data in order to determine, as accurately as possible, which cells are (even partially) occupied by obstacles, and which are (completely) empty, and thus suitable for robot navigation. In this manner, we can divide the set U into the set of empty cells E and the set of occupied cells O. It is possible due to the presence of uncertainty to provide only an estimate, of which cells belong to the set E and which ones belong to the set O. A compact way to represent this estimate is through a grey-level navigation map N, in which to each cell c_j from U a real number $\nu(c_j) \in \langle 0, 1\rangle$ is assigned, which incorporates the information about c_j gathered from R. The interpretation as well as the computation of N depends on the particular method chosen for managing uncertainty. The higher values in navigation map N denote the higher belief that the given cell is occupied.

2.1 Sonar uncertainty model

For modelling of the general behaviour of the sonar sensor in angular and range resolution, independently of the selected approach, an *angular radiation* function f_a and a *radial modulation* function f_d are introduced [3, 6]. Since the intensity of the ultrasonic waves decreases to zero at the borders of the radiation cone, the degree of certainty of each assertion (empty, occupied) is assumed to be higher for points close to the beam axis. This is realised by the angular modulation function

$$f_a(\vartheta) = \begin{cases} P(\vartheta) & 0 \le |\vartheta| \le 12.5^\circ \\ 0 & |\vartheta| \ge 12.5^\circ \end{cases}, \tag{2}$$

where $P(\vartheta)$ is the radiation directivity function (1). With an increase of the distance ρ of cell c_j from the sensor, the confidence for the assertion empty/occupied decreases. This fact is modelled by the radial modulation function

$$f_d(\rho) = 1 - \frac{\tanh\big(2(\rho - \rho_\nu)\big)}{2}\,. \tag{3}$$

The parameter ρ_ν is called the *visibility radius*, which defines the distance from the sensor where certainty continuously proceeds to uncertainty [3].

2.2 Probabilistic approach

Methods that make use of Bayesian estimation are the most common data fusion methods in occupancy grid creation [2, 5]. With this approach each cell stores a probable estimate of the occupancy of that cell in the form of a *state variable* $s(c_j)$. This variable is defined as an independent discrete random variable with two states, occupied and empty (O and E), *ie*, there is no relationship between the states of two cells c_j and c_i, even if they are adjacent [2]. Each cell c_j of the grid stores the probability of being occupied by the obstacle and the goal is the computation of that probability on the basis of measurements R. The cell states are exclusive and exhaustive and satisfy the condition

$$P[s(c_j) = O] + P[s(c_j) = E] = 1 \tag{4}$$

for all cells from U.

On the basis of [8], we propose the following sensor model to interpret the measured range data

$$p\big[r|s(c_j) = O\big] = p_1\big[r|s(\rho, \vartheta) = O\big] + p_2\big[r|s(\rho, \vartheta) = O\big] \tag{5}$$

$$p_1\big[r|s(\rho, \vartheta) = O\big] = \begin{cases} (1-\lambda)(0.5 - p_E)\,, & 0 \le \rho < r - 2\Delta r\,, \\ (0.5 - p_E)\Big[1 + \lambda\Big(\big(\frac{r-2\Delta r-\rho}{\Delta r}\big)^2 - 1\Big)\Big], & \\ & r - 2\Delta \le \rho < r - \Delta r\,, \\ \lambda(p_O - 0.5)\Big(1 - \big(\frac{r-\rho}{\Delta r}\big)^2\Big), & r - \Delta r \le \rho < r + \Delta r\,, \\ 0\,, & \rho \ge r + \Delta r\,, \end{cases} \tag{6}$$

$$p_2\big[r|s(\rho, \vartheta) = O\big] = \begin{cases} p_E\,, & 0 \le \rho < r - \Delta r\,, \\ 0.5\,, & \rho \ge r - \Delta r\,. \end{cases} \tag{7}$$

The constant factors p_E and p_O are the minimum and maximum values reached by the sensor model function and they hold the condition $p_E + p_O = 1$, r is a given range reading, $2\Delta r$ is the width of the area considered to be "proximal" to the arc of radius r, ρ is the distance c_j from the sensor, ϑ represents the angular distance between the axis of the radiation cone and the cell c_j, and $\lambda = f_a(\vartheta) f_d(\rho)$.

The sequential updating formulation of Bayes' theorem allows the incremental composition of sensory information. For a current estimate $P\big(s(c_j)=O|r_1,\dots,r_{n-1}\big)$ of the state of a cell c_j based on the observations $R=\{r_1,\dots,r_{n-1}\}$, and a new observation r_n, the improved estimate is given by

$$P\big(s(c_j)=O|r_1,\dots,r_n\big)= \frac{p\big(r_n|s(c_j)=O\big)P\big(s(c_j)=O|r_1,\dots,r_{n-1}\big)}{\sum\limits_{X\in\{E,O\}}\big(r_n|s(c_j)=X\big)P\big(s(c_j)=X|r_1,\dots,r_{n-1}\big)} \tag{8}$$

and $X\in\{E,O\}$. $P\big(s(c_j)=X|r_1,\dots,r_{n-1}\big)$ is the estimate of the cell state on the basis of measurements $r_1,\dots,r_{n-1}$ and $p\big(r|s(c_j)=X\big)$ is determined from the sensor model (5) considering (4). For the initial cell state the probability estimates are used with the maximum entropy $P\big(s(c_j)=E\big)=P\big(s(c_j)=O\big)=0.5$ [2]. With these initial values the state of cell is set to "unknown". With the probability theory approach, the navigation map N is obtained assigning $\nu(c_j)=P(s(c_j)=O|r_1,\dots,r_n)$.

2.3 Fuzzy logic approach

The basic concept of the methodology, that makes the use of fuzzy logic in the building of certainty grids from sonar readings, lies in the definition of empty and occupied spaces as fuzzy sets over the universal set U [6]. The sets are denoted as E and O, and their membership functions are μ_E a μ_O. The task of a map generating system is to assign for each cell c_j from U two values $\mu_E(c_j)$ and $\mu_O(c_j)$ from interval $\langle 0,1\rangle$, which quantify the possibility of the cell of belonging to an obstacle or to empty space. As the sets E and O are not complementary in the fuzzy context, partial membership to both fuzzy sets for c_j is possible. This allows us to identify areas where sonar observations have provided conflicting or insufficient information.

The following sensor models are used for values determination of membership functions $\mu_E(c_j)$ and $\mu_O(c_j)$ for c_j [6]:

$$f_e(\rho,r)=\begin{cases} k_e\,, & 0\le\rho<r-\Delta r\,,\\ k_e\big(\frac{r-\rho}{\Delta r}\big)^2, & r-\Delta r\le\rho<r\,,\\ 0\,, & \rho\ge r\,,\end{cases} \tag{9}$$

$$f_o(\rho,r)=\begin{cases} 0\,, & 0\le\rho<r-\Delta r\,,\\ k_o\Big(1-\big(\frac{r-\rho}{\Delta r}\big)^2\Big), & r-\Delta r\le\rho<r+\Delta r\,,\\ 0\,, & \rho\ge r+\Delta r\,,\end{cases} \tag{10}$$

Here ρ is the distance from the sensor, $k_e\le 1$ and $k_o\le 1$ are two constants corresponding to minimum and maximum values attained by the functions, $2\Delta r$ is the width of area considered to be "proximal" to the arc of radius r.

For each range measure it is possible inside the radiation cone to define the fuzzy set of empty cells $E^{\{r\}}$ and the fuzzy set of occupied cells $O^{\{r\}}$ by two membership functions as follows:

$$\mu_E^{\{r\}}(c_j)=f_a(\vartheta)f_d(\rho)f_e(\rho,r)\,, \tag{11}$$

$$\mu_O^{\{r\}}(c_j)=f_a(\vartheta)f_d(\rho)f_o(\rho,r)\,, \tag{12}$$

where ρ and ϑ are the polar co-ordinates of the cells associated with the sensor.

The building procedure of a fuzzy occupancy grid using (11) and (12), is made by using a fuzzy union operator [6]

$$E^{\{r_1,\dots,r_{i+1}\}}=E^{\{r_1,\dots,r_i\}}\cup E^{\{r_{i+1}\}} \tag{13}$$

$$O^{\{r_1,\dots,r_{i+1}\}}=O^{\{r_1,\dots,r_i\}}\cup O^{\{r_{i+1}\}}. \tag{14}$$

At the beginning a complete ignorance about a state of cells is assumed, $\mu_E=\mu_O=0$, and therefore $E^{\{\emptyset\}}=O^{\{\emptyset\}}=\emptyset$ for all cells in U.

The navigation map can be built by properly combining the two sets E and O. As already noted, these two sets do not contain complementary information, and consequently they can be combined to identify areas where the available information is either conflicting or insufficient. The fuzzy intersection of E and O is the set of *ambiguous* cells A, whose elements are both "empty" and "occupied", with the corresponding membership value representing the degree of contradiction $A=E\cap O$. The set of *indeterminate* cells I, whose elements are neither "empty" nor "occupied", is computed as $I=\overline{E}\cap\overline{O}$. A conservative map S of the *safe* cells is obtained by "subtraction" of the *occupied*, the *ambiguous* and the *indeterminate* cells from the *very empty* ones as follows $S=E^2\cap\overline{O}\cap\overline{A}\cap\overline{I}$. The squaring the value of the membership function E emphasises the difference between low and high values. According to the fuzzy logic terminology, it is the application of the linguistic modifier "very" to the "empty" concept [6]. The navigation map N corresponds to the fuzzy map of *dangerous* cells D, which must be avoided during the robot motion [3]. It is computed as $D=\overline{S}$ and thus $\nu(c_j)=\mu_D^{\{r_1,\dots r_n\}}(c_j)$.

For the above applied operations on fuzzy sets, the following operators are suitable [6]: $\mu_{\overline{A}}(x)=1-\mu_A(x)$ as a complementation operator, the bounded product

$$\mu_{A\cap B}(x)=\max\{0,\mu_A(x)+\mu_B(x)-1\}$$

as a conjunction operator, and Dombi operator

$$\mu_\lambda\big(\mu_A(x),\mu_B(x)\big)= \frac{1}{1+\Big[\big(\frac{1}{\mu_A(x)}-1\big)^{-\lambda}+\big(\frac{1}{\mu_B(x)}-1\big)^{-\lambda}\Big]^{-\frac{1}{\lambda}}}$$

as a union operator.

2.4 Evidence theoretic approach

The evidence theoretic approach is based on the Dempster-Shafer theory of evidence. The theory of evidence is based on the definition of a set Θ of mutually exclusive and exhaustive elements called elementary events. The set Θ is also called the *frame of discernment*. Any subset of Θ is a composite event, or hypothesis. In our case the interesting element events for map building application are that the cell c_j is empty or it is occupied. One of the main concepts underlying D-S theory is that of *basic probability assignment*. A basic probability assignment function $m\colon 2^{\Theta} \to \langle 0, 1\rangle$ is used to define the current state of each cell in the grid. It also defines the information provided by a new sensor reading and defined by the sensor model.

In the case of an occupancy grid creation, it is necessary to determine for all cells c_j from U, on the basis of measurements R, the evidence that the cell c_j is empty or belongs to an obstacle. Thus the set of discernment $\Theta = \{E, O\}$, and the set of propositions $\Lambda = 2^{\Theta} = \{\emptyset, E, O, E \cup O\}$ are defined [3, 8]. The state of each cell c_j is defined by basic probability assignment corresponding to a range reading r, which can be directly obtained through the certainty functions (2, 3, 9, 10)

$$m_j^{\{r\}}(E) = f_a(\vartheta) f_d(\rho) f_e(\rho, r), \tag{15}$$

$$m_j^{\{r\}}(O) = f_a(\vartheta) f_d(\rho) f_o(\rho, r), \tag{16}$$

$$m_j^{\{r\}}(E \cup O) = 1 - m_j(E) - m_j(O), \tag{17}$$

and $m_j^{\{r\}}(\emptyset) = 0$. These assignments express the evidence that the cell located at (ρ, ϑ) belongs to the sets E , O , $E \cup O$ and $\emptyset$.

The evidence for more measured data can be updated by using the Dempster combination rule

$$\forall A \in \Lambda\,,\ A \neq \emptyset\,, \quad m_j^{\{r_1,\ldots,r_n\}}(A) = \frac{\sum\limits_{B,C \in \Lambda; B \cap C = A} m_j^{\{r_1,\ldots,r_{n-1}\}}(B) m_j^{\{r_n\}}(C)}{1 - \sum\limits_{B,C \in \Lambda; B \cap C = \emptyset} m_j^{\{r_1,\ldots,r_{n-1}\}}(B) m_j^{\{r_n\}}(C)}, \tag{18}$$

$m_j^{\{r_1,\ldots r_n\}}(\emptyset) = 0$. At the beginning of computation the values of basic probability assignments are set as follows $m_j^{\{\emptyset\}}(E) = m_j^{\{\emptyset\}}(O) = 0$, $m_j^{\{\emptyset\}}(E \cup O) = 1$, $\forall c_j \in U$, which means the total ignorance of the state of each cell. The navigation map N is computed as follows [3]

$$\nu(c_j) = m_j(O) + \frac{1}{2} m_j(O \cup E)\,.$$

3 COMPARISON OF MAP–MAKING ALGORITHMS

The interesting parameters of data processing algorithms for mobile robot mapmaking are the computational speed and the quality of the resultant navigation map. Further the relevant property of given algorithms is the exploited amount of memory. The comparison of computational speed can be done by straightforward comparison of the processing times for a given data set without difficulties. The objective comparison of a navigation map's quality is more problematic. Up to now there have been made several qualitative mapmaking algorithm comparisons [3, 8], but none of them has the quantitative results. We propose simple criterions that enable us to compare the results of the ultrasonic data processed by different algorithms in the effort to specify the suitable solution for a mapmaking system for a developed mobile robot.

The maps intended for mobile robots should reflect as accurately as possible the space configuration of the given environment. Representation of the empty area suitable for robot motion and the restraints that must be avoided for safe navigation are necessary with the maximum accuracy and certainty. The final navigation maps obtained by different data processing algorithms can be compared with concern to a certain gauge. The ideal navigation map of the environment, where the ultrasonic data was gathered, was chosen as an applicable gauge. The ideal navigation map can be created from the accurate positions and the dimensions of all visible walls and objects in the experimental scene by manual measurement or automatically by the mobile robot. However, this robot must be equipped with a sufficiently precise positioning system and the correct sensory device like a laser scanner.

The parameter of our interest in the map quality determination is the detection reliability of the barriers and the free space. It is indicated that the degree of inequality of the ideal and the measured navigation map is suitable as the quality criterion of this created map. It is computed by subtraction of the real and the ideal map. This measure can also be interpreted as an error of the cell's state estimation in the grid. In the ideal navigation map the value $\nu(c_{Oj}) = 1$ is assigned to every occupied cell c_{Oj}. These cells correspond to surfaces of the walls and the objects and so they are truly occupied. The value $\nu(c_{Ej}) = 0$ is assigned to the empty cells c_{Ej} that correspond to truly free space. The spare cells behind the walls in the ideal map have the unknown state due to their invisibility to the sensory system and they will not be regarded in the criterion computation.

The criterion of detection reliability for occupied space is assigned as MQM_O (Map Quality Measure for occupied cells). It is calculated as the sum of the absolute differences between the values $\nu(c_j)$ and $\nu(c_{Oj}) = 1$ of the created and ideal map. The computation is done for all occupied cells c_O of ideal map. The resultant value is consequently averaged by the number of the occupied cells Nc_O of the ideal map. In this manner we obtain the

mean value of obstacle detection error. It characterises the obstacle detection performance of a concrete algorithm for the given map and enables us to compare the results for different maps. The smaller values of this criterion denote better approximation of the ideal map by the generated one and thus the better estimation of the obstacle boundaries. The criterion of detection reliability for empty space is assigned as MQM_E (Map Quality Measure for empty cells) and its calculation is done analogically as for the occupied cells. It is computed as the sum of the absolute differences of the created $\nu(c_j)$ and ideal $\nu(c_{Ej}) = 0$ map for all empty cells of the ideal map. The resultant sum is averaged finally by the number of the empty cells Nc_E of the ideal map. This final value can be interpreted as the mean value of the empty space detection error. As well as for the MQM_O criterion, the smaller values denote better empty space detection. Then final equations for MQM_O and MQM_E calculation are given as follows:

$$MQM_O = \frac{\sum\limits_{\forall c_O} |\nu(c_j) - \nu(c_{Oj})|}{Nc_O}, \tag{19}$$

$$MQM_E = \frac{\sum\limits_{\forall c_E} |\nu(c_j) - \nu(c_{Ej})|}{Nc_E}. \tag{20}$$

The overall map quality can be expressed by the difference of the created and ideal map for all empty and occupied cells of the ideal map. We assign it as MQM and it is computed analogically like the criterions for occupied and empty spaces. The criterion MQM represents the overall space detection error of the map. More accurately generated maps are represented by smaller values of MQM. The criterion is given by following relation

$$\begin{aligned} MQM &= \frac{\sum\limits_{\forall c_{(O,E)}} |\nu(c_j) - \nu(c_{(O,E)j})|}{Nc_{(O,E)}} \\ &= \frac{\sum\limits_{\forall c_O} |\nu(c_j) - \nu(c_{Oj})| + \sum\limits_{\forall c_E} |\nu(c_j) - \nu(c_{Ej})|}{Nc_O + Nc_E} \\ &= \frac{MQM_O Nc_O + MQM_E Nc_E}{Nc_O + Nc_E}. \end{aligned} \tag{21}$$

4 SONAR DATA ACQUISITION

It is obvious that the results of comparison need not be generally strictly identical for different surroundings. This fact is given by the intrinsic properties of particular algorithms and by reflectional properties of the objects in the environment. Hence it is desirable for the general comparison of the algorithms to choose the space with the broadest possible scale of objects with different surfaces. So the performance of the map generating algorithms was tested in two different indoor environments. The first is a long hallway Figs. 1, 2 and the second is a relatively large vestibule in our department Fig. 3. Out of several aspects they represent well enough the indoor office-like environment. The walls of the hallway have relatively different reflection properties. They are formed by furniture with a smooth splint surface on one side and by common plaster on the other one. Both endings of the hallway are enclosed with wide glass doors. On both sides of the hallway are several doors with glass filling. In addition, they are fairly deeply embedded on one side into the wall, some up to 65 cm. This fact enables us to test the ability of compared algorithms to find and to identify a narrow corridor in the wall. Furthermore one of the doors was open during the experiment. The length of the hallway is about 20 m and its width is approximately 1.8 m. The walls in the vestibule have very different the ultrasound reflection properties too. They are constituted from common plaster, wood, glass bulletin boards and wide glass alternative metal doors. Some of the doors are situated deeply in the walls. Three artificial obstacles of various shapes with equal surfaces were placed in the centre of the vestibule. The dimensions of the vestibule are approximately 11×6 m.

The data gathering was performed with a movable platform equipped with the Polaroid sensor device at the top. The sensor device was able to rotate in full, to an angle of $360°$. The measuring locations were evenly distributed with an interval of 0.5 m to obtain a good coverage of the environment. Along the hallway were placed 39 and in the vestibule 205 measuring locations. At each location a data set composed of the 400 measurements was collected by the sensor rotation with a fixed step $0.9°$.

The first universal set U_1 for the hallway has 300×100 cells and the second universal set U_2 for the vestibule has 220×160 cells of the cell size $\delta = 0.1$ m. The parameter $p_O = 0.6$ was used for the probabilistic approach and $k_e = 0.25$ and $k_o = 0.45$ for the evidence theoretic approach. For the fuzzy logic approach parameters with the following values $k_e = 0.25$, $k_o = 0.05$ and $\lambda = 0.5$ for the Dombi operator were used. The values of the parameters $\rho_\nu = 1.2$ m and $\Delta r = 0.15$ m were identical for all three methods.

The algorithms were implemented in C language on PC equipped with an 2500MHz Athlon processor running under Linux. The resulting navigation maps are depicted as grey scale images at Figs. 1–3. The colour in the images indicates the level of confidence in the proposition, that the corresponded environment area is occupied with the obstacles. The lighter areas $\nu(c_j) \to 0$ represent the empty cells and the darker areas where $\nu(c_j) \to 1$ represent occupied cells. The boundaries of walls are represented with the white lines. The measuring locations are depicted as a small crosses. The background colour represents entire ignorance about the state of the cells in the map. For the probabilistic and evidence theoretic methods the background colour is grey and for the fuzzy logic method it is the colour black.

5 EXPERIMENTAL RESULTS

The comparison of the three main approaches to the creation of the navigation grid maps from the sonar range measurements was realized in two different real indoor environments. In every environment one data set with the 400 measurements per position was obtained. The tests were done on subsets extracted from two main data sets. The subsets contained 10, 16, 20, 25, 40, 50, 80 and 100 measurements per measuring position. The reason was to find out the effect of different number of measurements on the final maps. Examples of the resultant navigation maps are shown in Figs. 1–3. The first and second figure show the navigation maps of the first testing environment constructed with the probabilistic and fuzzy logic approach and Fig. 3 represents the navigation map of the second environment created by the evidence theoretic approach. These maps were built from the data subset with 40 measures per location.

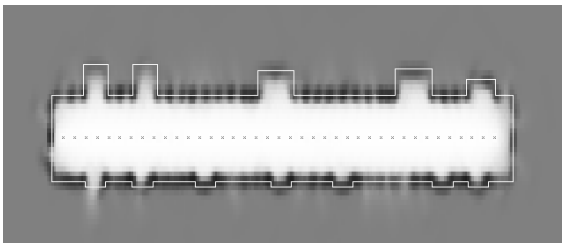

Fig. 1. Navigation map of the first environment obtained by the probability approach..

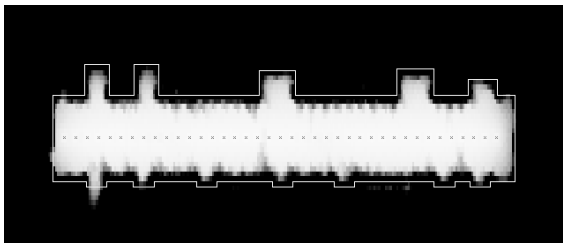

Fig. 2. Navigation map of the first environment obtained by the fuzzy logic approach.

The contours of the testing environments proved to identify all three methods sufficiently. The probabilistic and evidence theoretic approaches were able to find the boundaries of the occupied space relatively accurately. The contours in maps continuously copy the real ones, and the boundaries are extended about two cells (Figs. 1, 3). The fuzzy logic approach defines the profile of the hallway with little higher inaccuracy. Streaks of darker cells appear with a higher certainty of their occupancy in empty space of the map (Fig. 2). On the other hand this approach produces fewer areas of the empty cells behind the occupied ones belonging to the walls. This fact indicates the better robustness of the method against the multiple reflections. The open doors and narrow corridors embedded in the walls of the hallway were identified by all three approaches. Though the fuzzy algorithm narrowed them even more in the map and that fact might be a serious problem in the path planning process. The endings of the hallway with glass doors were identified fairly well. However the long readings resulted in a smaller degree of the certainty about the occupation of this area.

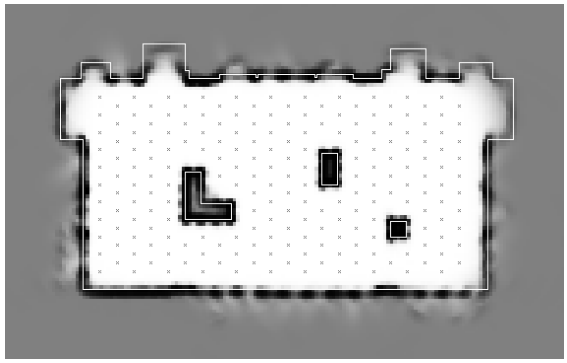

Fig. 3. Navigation map of the second environment obtained by the evidence theoretic approach.

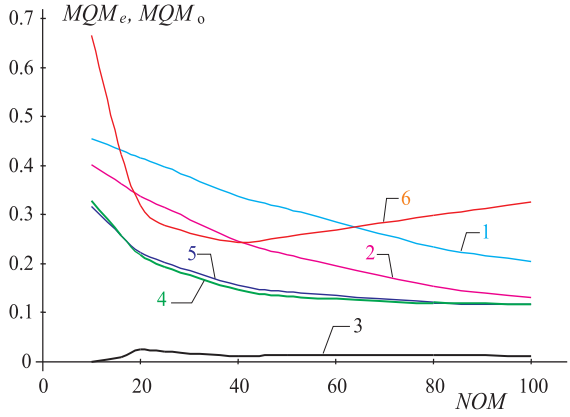

Fig. 4. Relation of the map quality measures on the number of measurements for the first environment. 1– MQM_O and 4– MQM_E for probability, 2– MQM_O and 5– MQM_E for evidence theoretic and 3– MQM_O and 6– MQM_E for fuzzy logic algorithm

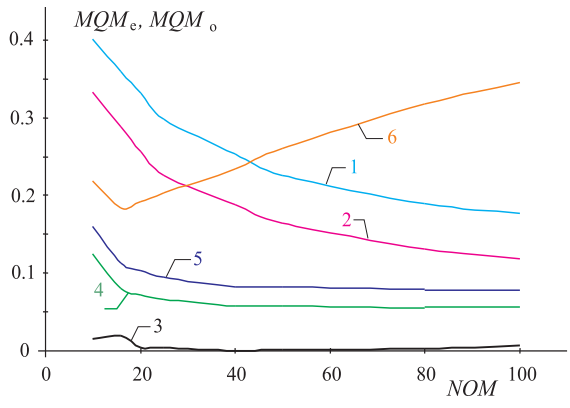

Fig. 5. Relation of the map quality measures on the number of measurements for the second environment. 1– MQM_O and 4– MQM_E for probability, 2– MQM_O and 5– MQM_E for evidence theoretic and 3– MQM_O and 6– MQM_E for fuzzy logic algorithm

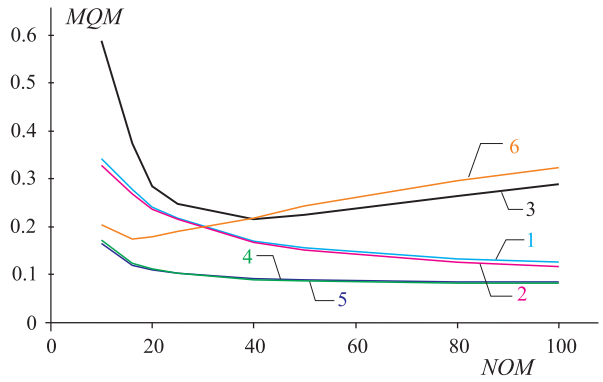

Fig. 6. Dependency of the overall map quality measure on the number of measurements for both experiments. 1–probability, 2–evidence theoretic and 3–fuzzy logic algorithm for the first environment 4–probability, 5–evidence theoretic and 6–fuzzy logic algorithm for the second environment

The obtained values of the map quality measures for maps generated by all three methods along with map computation times are displayed in tables Tabs. 1–3. The functional dependencies of MQM_O and MQM_E criterions on the number of measurements (NOM) for both experimental environments are depicted in Figs. 4 and 5. The graphs of the resultant values for the overall quality criterion MQM are shown in Fig. 6.

The algorithms performance analysis is done on the basis of the computed values of the empty and occupied space detection criterions. The empty space detection ability has an essential influence on the overall map quality. It is caused by the generic geometric properties of the environments and the definition of the criterion. Consequently the values of the overall quality criterion and their trends are close to the values of the criterion for the empty space detection. The experiments in the two different environments showed the universal properties of the given algorithms. The results depicted in Figs. 4 and 5 show that the equivalent parameters have very similar trends for both data sets. However, there is a noticeable drift of all the curved lines for the first environment towards the higher error values in comparison with the curves for the second one. This fact is caused by the geometry of the experimental space. If the sensor is directed along the hallway, then the hallway walls reflect the wide-angle sonar beam back to the sensor. So the considerably narrow hallway causes the occurrence of illusory objects in the empty space. Therefore the geometry of the experimental space and the wide sonar beam disable to achieve higher quality of the final navigation map for the first environment. The second general difference between the graphs is the slower regress of the error criterions for the first experiment along with the growing number of measurements (NOM). This fact is noticeable for the probabilistic and evidence theoretic algorithm and this property is apparently caused by the geometry of the environment too. These two methods are fairly similar in regard to the concept of the measured data integration to the map and the navigation map creation. The information about empty and occupied space is handled equivalently in the process of the navigation map creation. Therefore they produce similar results as opposed to the fuzzy logic method. In their case more information about the environment produces better quality map. Though this fact is not valid for the fuzzy logic approach. In this case the situation is more complicated and shapes of the graph curves are completely different. The quality of fuzzy map as a function of NOM is at first rising for a small number of measurements, but it goes evenly down for higher amounts of measurements. This interesting feature is caused by the algorithm intrinsic data treatment. The fuzzy navigation map creation imposes the main emphasis on the clearly empty area for the purpose of the maximum safe robot motion. Along with more measurements, more cumulative erroneous information occurs in the cells along the walls. These cells are then evaluated as dangerous to the robot motion and the walls are going to be wider in the navigation map. So the safe area for the robot navigation in the map becomes smaller and so the map quality decreases. It can be said that it is not a very useful property, if more sensed information about the environment produces less accurate navigation maps. On the other hand, a finite amount of measurements are needed for the creation of a fuzzy map with the maximum quality. So the exploration of the environment can be done more quickly for the best achievable results. As we can see, the number of measurements for the lowest map error varies for different environments and it is dependent on the environment properties. Thus the optimal fuzzy map is generated from 40 measures per position for the first experiment and from 16 for the second one.

As we can see in the Figs. 4–6 the performance comparison of the grid mapmaking methods is not a straightforward problem. The best result for empty space detection in the cases of both experimental environments was achieved by the probability algorithm. The evidence theory method result was only minimally worse. On the other hand, the curves representing the performance results of the empty space detection for the fuzzy logic approach lye highest on both graphs and their values are moderately worse when compared to the previous algorithms. The determination of the best result is a little more complicated in the case of the ability to detect the occupied space. As can be seen in both figures, the curve with the far lowest values of the map error belongs to the fuzzy approach. However this almost perfect obstacle detection, even with only the few measurements, is false. This feature results from the computation concept of the navigation map, which is the map of "dangerous" cells D. Also the weakly observed cells along with the occupied ones are marked as unsuitable for the robot motion in this map. These cells are assigned to the occupied ones in the navigation map. The poorly observed contours of the environment were regarded as the obstacles already at the beginning of exploration, when only the few measurements were realized. Consequently the evidence theoretic approach really has the highest ability to detect the occupied space in both experimental environments. The

Table 1. Map quality measures and computing times for the probabilistic algorithm.

NOM	Environment 1				Environment 2			
	MQM_O	MQM_E	MQM	$Time$ (ms)	MQM_O	MQM_E	MQM	$Time$ (ms)
10	0.454764	0.327071	0.342077	170	0.400941	0.14788	0.164687	1570
16	0.432238	0.257822	0.278388	280	0.358958	0.102778	0.120025	2540
20	0.414704	0.218772	0.241876	370	0.331746	0.094837	0.110704	3130
25	0.397145	0.193084	0.217146	450	0.298188	0.088917	0.103006	3840
40	0.338093	0.14656	0.169145	710	0.253679	0.080135	0.091818	6190
50	0.312098	0.13409	0.15508	900	0.225456	0.080185	0.089965	$7660k$
80	0.23481	0.120245	0.133754	1430	0.189868	0.078173	0.085693	12330
100	0.204742	0.116874	0.127235	1800	0.177068	0.078212	0.084867	15390

Table 2. Map quality measures and computing times for the evidence theoretic algorithm.

NOM	Environment 1				Environment 2			
	MQM_O	MQM_E	MQM	$Time$ (ms)	MQM_O	MQM_E	MQM	$Time$ (ms)
10	0.402206	0.317291	0.32727	180	0.332379	0.160367	0.171791	1590
16	0.363511	0.256771	0.269357	290	0.288131	0.11243	0.124258	2560
20	0.336315	0.223099	0.236449	380	0.256814	0.102659	0.112983	3160
25	0.313739	0.202338	0.215474	460	0.22578	0.094248	0.103104	3920
40	0.245925	0.15718	0.167645	730	0.187719	0.082475	0.08956	6320
50	0.219015	0.142851	0.151831	920	0.164133	0.081826	0.087368	7820
80	0.154905	0.122143	0.126006	1440	0.131364	0.079144	0.08266	12550
100	0.131171	0.116092	0.11787	1820	0.118806	0.079107	0.08178	15670

Table 3. Map quality measures and computing times for the fuzzy logic algorithm.

NOM	Environment 1				Environment 2			
	MQM_O	MQM_E	MQM	$Time$ (ms)	MQM_O	MQM_E	MQM	$Time$ (ms)
10	0	0.665125	0.586964	230	0.015538	0.218225	0.204763	2070
16	0.008797	0.421999	0.373276	370	0.020159	0.184495	0.173431	3350
20	0.024968	0.319848	0.285077	500	0.004236	0.192756	0.18013	4150
25	0.021269	0.276876	0.246736	590	0.0035	0.202914	0.189489	5090
40	0.012511	0.243611	0.216361	950	0.000597	0.234301	0.218568	8230
50	0.014905	0.253616	0.225469	1210	0.000861	0.260436	0.24296	10190
80	0.013937	0.298425	0.264879	1910	0.003212	0.317222	0.296082	16410
100	0.011493	0.32681	0.289629	2420	0.006289	0.345834	0.322975	20510

probability approach has the higher values for the equivalent criterion. Hence it can be summarised that, from the measured distance values, the best quality maps are generated by the evidence theoretic approach. This fact is confirmed also by the smallest values of the overall quality criterion MQM.

The computation times for all the experiments are shown in tables Tabs. 1–3. It can be seen, that the fastest map-building algorithm is based on the theory of probability. The second minimal computation times are only a little greater and they belong to the evidence theoretic algorithm. The slowest approach is based on the fuzzy set theory. The probability method also has the lowest memory consumption. The other two methods have higher memory requirements.

7 CONCLUSION

The occupancy grid map quality measures were introduced. The aim was the determination of the qualitative properties of given map building algorithms. Their computation complexity was the second parameter of our interest. On the basis of the obtained results the comparison of these methods was done. So the suitable solution can be chosen for the mapmaking system of a mobile robot. The designed map quality criterions are capable of mea-

suring and consequently of comparing the performance of the algorithms individually for the empty and occupied space of the environment. In this manner the influence of the objects surfaces and the erroneous readings on the final maps generated by individual methods can be investigated for example. It is also possible to optimise intrinsic parameters of the algorithms for the best results in the given robot working environment. The experiments were done with the data collected in two real indoor environments. The reason for the map computation on more data sets was the ambition to investigate how the different number of measures affects the degree of evidence about occupied and empty space. Several interesting features of the investigated data processing methods were revealed. The comparison of the three principal approaches for creation of the occupancy grids, intended for the mobile robots navigation tasks, shows us more or less their advantages and disadvantages as well as offering topics for future research.

References

[1] BORENSTEIN, J.—EVERETT, B.—FENG, L.: Navigating Mobile Robots: Systems and Techniques, A.K. Peters, Ltd., Wellesley, MA, 1996.

[2] ELFES, A.: Using Occupancy Grids for Mobile Robot Perception and Navigation, Computer Magazine (June 1989), 46–57.

[3] GAMBINO, F.—ORIOLO, G.—ULIVI, G.: A Comparison of Three Uncertainty Calculus Techniques for Ultrasonic Map Building, In: SPIE 1996 Int. Symp. on Aerospace-Defence Sensing and Control, Orlando, Fl, 1996, pp. 249–260.

[4] KORTENKAMP, D.—BONASSO, P. R.—MURPHY, R.: Artificial Intelligence and Mobile Robots, Case Studies of Successful Robot Systems, AAAI Press/The MIT Press, 1998.

[5] MORAVEC, H. P.: Certainty Grids for Mobile Robots, Proceedings of the NASA/JPL Space Telerobotics Workshop, vol. 1, 1987, pp. 307–312.

[6] ORIOLO, G.—ULIVI, G.—VENDITTELLI, M.: Fuzzy Maps: A New Tool for Mobile Robot Perception and Planning, Journal of Robotic Systems **14** No. 3 (1997), 179–197.

[7] Polaroid (1992). Polaroid Ultrasonic Ranging System Handbook — Application Note/Technical Papers.

[8] RIBO, M.—PINZ, A.: A Comparison of Three Uncertainty Calculi for Building Sonar-Based Occupancy Grids, Robotics and Autonomous Systems **35** No. 3–4 (2001), 201–209.

[9] TOMAN, M.: Ultrasound for Spatial Measurements, AT&P JOURNAL plus2, **7,** (2001), 66–75. (in Slovak)

Received 7 March 2006

Jaroslav Hanzel (Ing), received the Ing degree in 2000 in Automation and Control from the Slovak University of Technology, Faculty of Electrical Engineering and Information Technology in Bratislava. Since 2003 he is a research worker at the department of Automation and Control. He works in the field of autonomous navigation of the mobile robots. His main research interests are the acquisition and processing of data from sensors, algorithms for robot navigation and artificial intelligence methods applicable in the mobile robotics.

Ladislav Jurišica (Prof, Ing, PhD), received the Ing degree in 1964 and PhD degree in 1974, both in Electrical Engineering (Automation and Control) from the Slovak University of Technology, Faculty of Electrical Engineering in Bratislava. Since 1965 he was a research worker, then appointed Associate Professor in 1979. Since 1994 he is Full Professor at the Faculty of Electrical Engineering and Information Technology. His main interests are the systems of motion control, and the control of robotic systems. At present he is the leader of a research project in this field.